Petroleum Res. J. Vol. 17 (2005); P. 67–72, 11 Figs.

Evaluation of Imidazoline-based Inhibitors for Oil Environment by Means of Advanced Eelectrochemical Methods

G. Gusmano*, G. Montesperelli**, P. Labella***, A. Privitera*** and S. Tassinari***

تقييم مثبط التآكل المكون من مادة إميدازولين لإستخدامه في البيئة النفطية بإستخدام أساليب كهروكيميائية متقدمة

ج. قوسمانو وج. مونتيسبيريلي وب. لابيلا وأ. بريفيتيرا وس. تاسيناري

تتطرق هذه الورقة الي النتائج الأولية لإختبارات تقييم نشاط مثبطات التآكل المكونة من مادة إميدازولين بإستخدام طيف المعاوقة الكهروكيميائية بالإضافة الي طرق كهروكيميائية تقليدية أخرى.

أجريت الإختبارات على عينات من الفولاذ الطري نوع AISI 1040 مغمورة في محلول يحاكي تركيب الطور المائي المصاحب للزيت الخام أثناء عمليات إنتاج ونقل النفط أي أنه شديد الملوحة ويحتوي علي غاز ثاني أكسيد الكربون ويوجد في بيئة لاتحتوي على الاوكسجين وعند درجة حرارة 40 درجة مئوية.

تم إختبار تركيبتين مختلفتين للمثبط. حللت معطيات طيف المعاوقة الكهروكيميائية بواسطة الدوائر المكافئة وقد مكنت الإختبارات الكهروكيميائية التقليدية من إثبات آليات وأنماط نشاط مختلفة وذلك حسب المثبط.

Abstract: *In this paper preliminary results of tests for the evaluation of the activity of imidazoline-based corrosion inhibitors by means of Electrochemical Impedance Spectroscopy (EIS) and other traditional electrochemical methods are reported. Tests have been carried out on AISI 1040 mild steel specimens immersed in solution simulating the composition of aqueous phase during oil production and transportation: high salinity, presence of CO_2, anaerobic environment, temperature 40 °C. Two different inhibitor formulations were tested.*

EIS data have been analysed by means of equivalent circuits. The electrochemical tests permitted to evidence different mechanisms and activity depending on inhibitor formulation.

* Dipartimento di Scienze e Tecnologie Chimiche, Universita di Roma "Tor Vergata".

** Dipartimento di Fisica ed Ingegneria dei Materiali e del Territorio Universita Politecnic Marche.

*** Ondeo-Nalco Italia s.r.l.

INTRODUCTION

The environmental conditions in oil fields can be very different but they could be assumed follow: anaerobic conditions, high concentration of CO_2 (often close to saturation), high salinity, variable concentration of sulphide ions[1-2] and high temperature.

Depending on composition, different forms of corrosion can take place in oil and gas wells and flow lines[3]. Amongst them, CO_2 corrosion, usually called sweet corrosion, is one of the most severe.

The main method of protection all petrochemical facilities in the world is the use of inhibitors, because of their great flexibility by adjusting their concentration in relation to environmental corrosivity.

The most effective corrosion inhibitors for oil and gas pipeline application are the fatty acid imidazoline. About 90% of inhibitor used by oil companies is based on the use of aliphatic long chain diamines or imidazolines. The action mechanism of imidazolines, whose general structure is depicted in Figure 1, is not well understood[4-8]. It has been reported that

imidazolines form a double layer on the metal surface and that their activity depends on the nature of the hydrocarbon tail, but many details have to be cleared, in particular regarding their action mechanism.

In this paper some results of a research program on the evaluation of two different imidazoline-based inhibitors are reported. In particular, tests on carbon steel specimen have been carried out by means of different electrochemical methods such as: Open Circuit Potential (OCP), Polarization Curves (PC), Linear Polarization Resistance (LPR) and Electrochemical Impedance Spectroscopy (EIS).

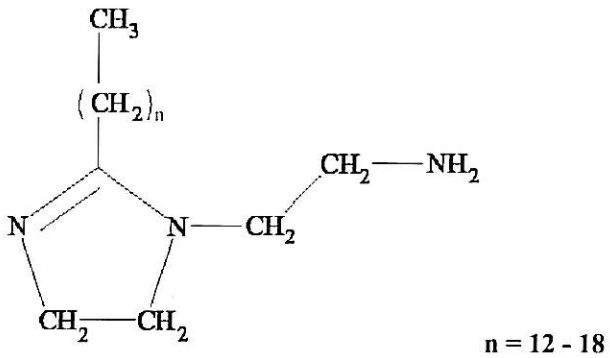


Fig. 1. General chemical structure of imidazolines used in this work.

EXPERIMENTAL

Tests have been performed on AISI 1040 cylindrical electrodes, 4 mm in diameter. Surface electrode was delimitated by enamel and the immersed area was 10.2 cm^2.

Tests were carried out in an unstirred solution of 30 g/l sodium chloride in which a constant CO_2 bubbling was performed throughout tests. A sealed cell was used with a vent to prevent over pressure. The cell was thermostat-controlled at 40° C and oxygen concentration was measured by an Orbisphere Laboratories Model 2713 probe, and kept below 10 ppb during all the tests.

Inhibitors were a commercial mixture of imidazolines with an aliphatic chain varying between 12 and 18 carbon atoms, as shown in Figure 1. Two different inhibitors formulation, supplied by Ondeo-Nalco, at concentration of 25 or 50 ppm were used and their compositions are reported in Table 1. Inhibitor A contained acetic acid as salting agent whereas inhibitor B contain a mixture of acetic acid and thioglycolic acid. Blank tests were also performed.

EIS measurements were carried out at the OCP in the frequency range $5x10^{-3}$ -$5x10^{5}$ Hz with an A.C. signal of 5 mV by a Solartron 1260 Frequency Response Analyser (FRA) and a 273 E.G. & G. Princeton Applied Research Potentiostat-Galvanostat. Equivalent circuit evaluation of EIS data was performed by Z-Plot software (Scribner Ass.) using a Non Linear Least Squares (NLLS) algorithm.

Corrosion rate measurements were performed by Linear Polarization Resistance (LPR) method by an ADSE corrosimeter using a three-electrode corrosion probe.

Polarization Curves were performed with a scan rate of 4 mV/s.

Table 1. Composition of inhibitors (% Wt)

Components	Inhibitor A	Inhibitor B
Imidazolines	25	25
Acetic acid	6	3
Thioglycolic acid	-	3
Isopropanol	10	10
Water	balance	balance

RESULTS AND DISCUSSION

The OCP trend of specimens in inhibited solution (50 ppm) is shown in Figure 2, in which, as a comparison, the OCP for a blank test is also reported. OCP curves of tests in inhibited solution showed a clear ennoblement from the first hour of immersion. No relevant differences were detected between inhibitors A and B. After 4 hours, OCP kept a constant value in the range between -650 and -640 mV (Vs AgCl) for inhibited tests, while the blank test settled at about -710 mV.

Polarization curves were performed at the same condition. Figure 3 reports polarization curves of tests with inhibitor A at 50 ppm, immediately after the immersion and after 2 and 6 hours. Polarization

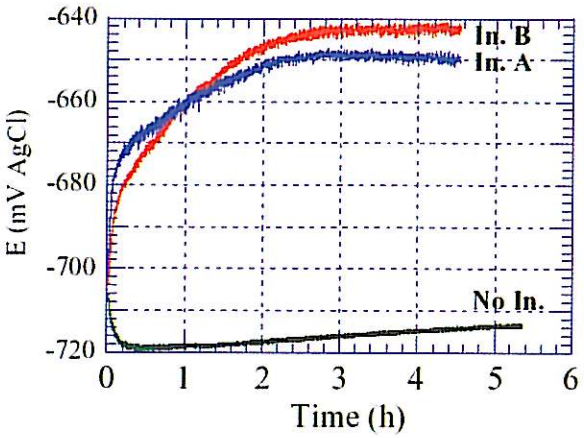


Fig. 2. OCP as a function of immersiontime (Inhibitor concentration: 50 ppm).

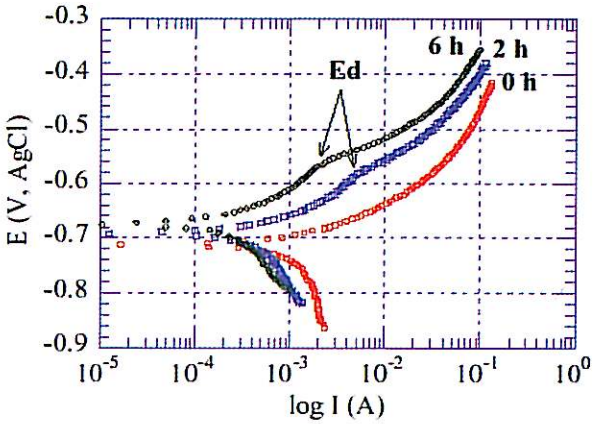


Fig. 3. Polarization curves for inhibitorA at 50 ppm, at different immersion time.

curves show an OCP shift towards anodic direction and the concurrent increase of both anodic ($\bullet_a$) and cathodic ($\bullet_c$) Tafel slopes with time, typical of adsorption inhibitors. Within the anodic part of curves collected after 2 and 6 hours of immersion, a slope variation can be detected, indicated by the arrow in Figure 3. This behaviour reveals the potential at which the film breakdown takes place and it is usually called desorption potential (E_d)[9].

A slight increase of E_d with time can be detected (from –584 to -557 mV). Data of polarization curves taken after 6 hours for both the inhibitors are summarised in Table 2.

Table 2. – $\bullet_a$, $\bullet_c$ and E_d after 6 hours

Blank Inhibitor A	Inhibitor B
•a (mV) •c (mV) Ed (mV)	93 130 129 318 217 89 - - 557 -439

Inhibitor B shows an increase of E_d, stronger than that observed for inhibitor A, thus indicating a higher film stability with respect to inhibitor A.

The results of LPR measurements, shown in Figure 4, demonstrate that corrosion rate for inhibitor

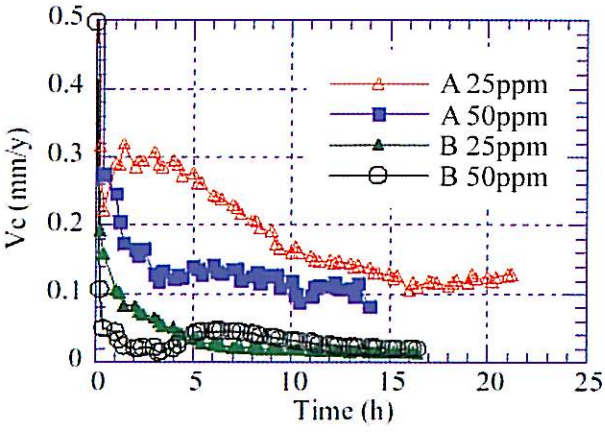


Fig. 4. Corrosion rates by LPR.

A at 25ppm settled at 0.15 mm/y after about 12 h of immersion, while for the same inhibitor at a concentration of 50 ppm reached a corrosion rate of 0.10 mm/y in a shorter time. The same measurements for inhibitor B showed corrosion rates lower than 0.02 mm/y after only 5 hours for both concentrations. LPR tests for blank tests gave an average corrosion rate of 1.40 mm/y.

EIS measurements were performed in three different conditions: without inhibitor and in the presence of inhibitors A and B at the concentrations of 25 and 50 ppm.

The analysis of EIS data, acquired during blank tests, shows that this system is described by a simple RC parallel equivalent circuit, as reported in Figure 5a, being R_s the electrolyte resistance, R_{ct} the charge transfer resistance and CPE_{dl} the double layer capacitance. No circuit element that can be related to the presence of any protecting film on metal surface was detected. No contribution from diffusion (Warburg impedance) was also detected, since the oxygen concentration within the cell was negligible. The equivalent circuit has been developed using Constant Phase Element (CPE) instead of real capacitance because of the semiarc depression in the Nyquist plot. The contribution of CPE to total impedance is given by $½ = Y_o (j\omega)^n$ in which Y_o is the admittance and n a parameter associated to the semiarc depression with respect to real axis. If n = 1, CPE contributes as an ideal capacitance.

R_{ct} values for blank test varied in the range between 10 and 20 Ohm, thus confirming the high corrosion rate V_c measured by LPR. C_{dl} was high, in the range 4-6 mF, due to the presence of a high charge concentration on electrode surface.

EIS spectra acquired in inhibitor A solution were described by the equivalent circuit of Figure 5b, in which two additional elements are present: the film resistance (Rf) and capacitance (CPE_f). This is a

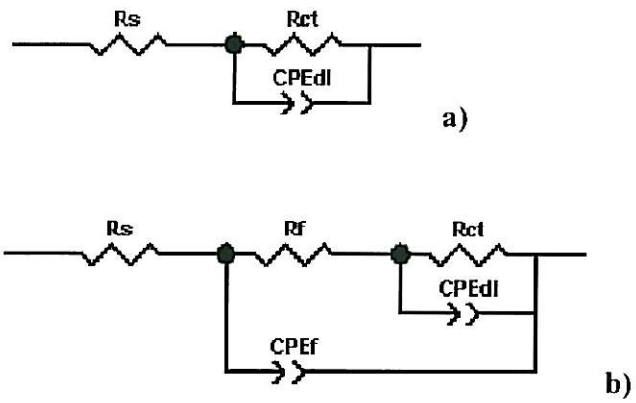


Fig. 5. Some of the equivalent circuits used in this paper.

generally accepted equivalent circuit to describe the corrosion behaviour of film-coated metals, where the metallic substrate is exposed to the electrolyte through the permeable defects (*e.g.* pores) present in the film[4-10].

The use of this equivalent circuit permitted a good simulation of the EIS data as shown in Figure 6 for a spectrum related to a test with inhibitor A at 50 ppm. The f^2 test and Weighted Sum of Squares (WSoS) values were respectively 4.2 10^{-4} and 3.6 10^{-2} for circuit 5b, thus confirming good fitting.

The use of equivalent circuits with NLLS-fit (an extension of least squares regression method) permitted to calculate the charge transfer and film parameters during test. According f^2 test (the square of the standard deviation between the original data and the calculated spectrum) and WSoS values, the error associated to circuit element estimation was always < 5 %. The first EIS spectra acquired few minutes after the immersion indicated only one semiarc that, on the basis of capacitance values, can be ascribed to charge transfer reaction. With increasing of immersion time, charge transfer characteristic moved towards low frequency and a strong increasing in total resistance was observed. After few hours of immersion, a second time constant was observed in the high frequency region (indicated by the arrow in Figure 6). This new time constant can be attribute to the imidazoline film formation. Figure 7 reports R_{ct} and R_f trend for a typical test in inhibitor A at 50 ppm.

R_{ct} and R_f have very similar trends characterized by a marked increase in the first part of the test, confirming that the film formation is fast. After 10 hours, R_{ct} settled at a constant value of about 1350 Ohm whereas the trend of R_f was still increasing.

Figure 8 reports, the trend of C_{dl} and C_f for the same test as Figure 7. C_{dl} and C_f show an inverse trend, with strong decrease for C_{dl} in the very first part of the test and a slight increase for C_f during the first 20 hours of the test. After that, both capacitances become constant and very close to a value of about 870 ^F.

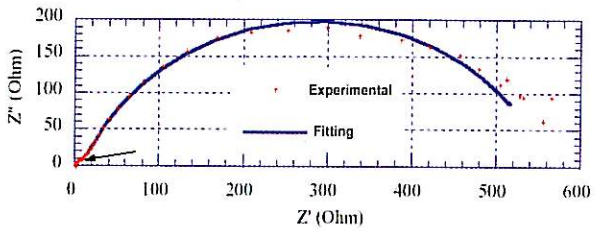


Fig. 6. Fitting of a typical Nyquist plot for a test with inhibitor A, using the equivalent circuit in figure 5b.

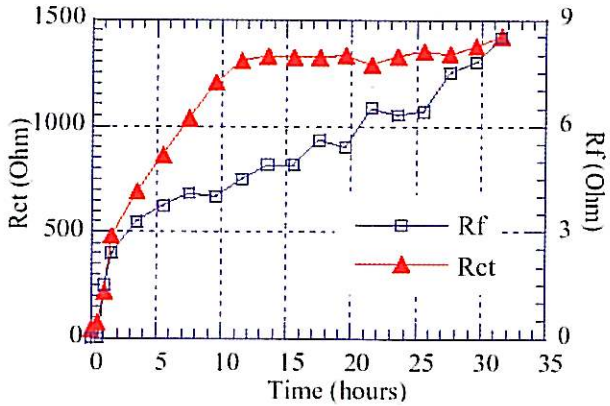


Fig. 7. R_{ct} and Rf trend as a function of time for a test in inhibitor A at 50 ppm.

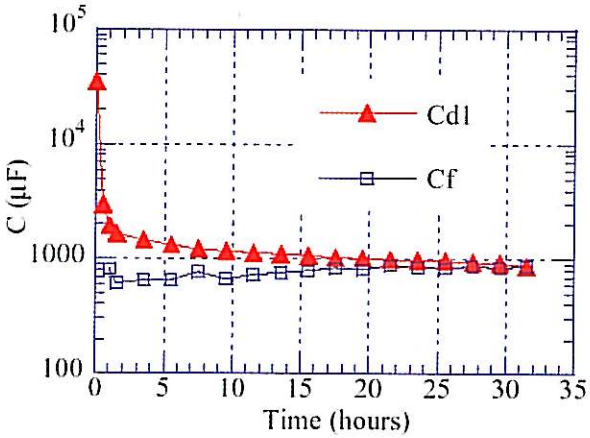


Fig. 8. C_{dl} and C_f trend as a function of time for a test in inhibitor A at 50 ppm.

EIS spectra, acquired on tests with inhibitor B, showed a more complex outline. Circuit in Figure 5b did not allowed to have good fit, thus suggesting a more complex film-metal interface structure with respect to inhibitor A. For this reason, the analysis of EIS data on inhibitor B required the addition of a new RC circuit as shown in Figure 9. This new RC circuit, whose parameters have been labeled R_z and C_z, can be ascribed to the effect of thioglycolic acid to film build up.

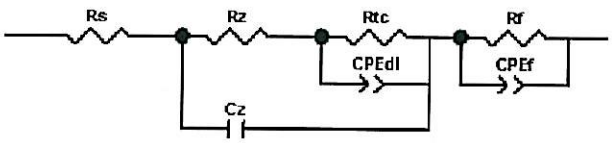


Fig. 9. Equivalent circuit used to fit EIS spectra on inhibitor B.

Resistance values as a function of immersion time are shown in Figure 10. R_{ct} and R_f have the same trend since both of them are related at the film formation. R_f is about one order of magnitude higher with respect to that of inhibitor A. As a consequence of this, R_{ct} reached a steady value of 3500. R_z gave a poor contribution to the total resistance (about 15•)

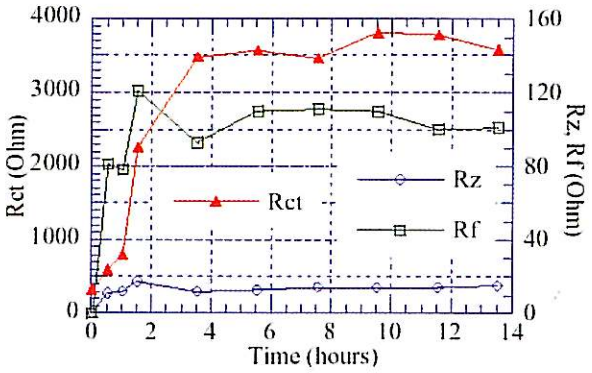


Fig. 10. R_{ct}, R_f and R_z as a function of time for a test in inhibitor B at 50 ppm.

and is essentially independent on time. As a first assumption, thioglycolic acid seems to be inaccessible by solution, acting as an inner layer and the very low R_z suggesting that it is not protective itself. It is well known that thioglycolic acid decompose in the presence of heavy metal to produce hydrogen sulfide and an FeS precipitation could be hypothesized.

C_{dl} has a trend very similar to that of inhibitor A: after a slight decrease, reached a constant value of 500 ^F. On the other hand, C_f decreases during first hours of immersion, probably because of the increasing of film thickness since the capacitance is inversely proportional to it.

C_z contribution is small and approximately unaffected by immersion time as well as R_f. It can be assumed that its effect takes place in the very first part of the film build up (Fig. 11).

As a general remark, EIS data suggest that the presence of thioglyc olic acid or of sulphides, coming from its decomposition, can influence the kinetic of imidazoline adsorption on metal surface, thus resulting in an improvement of activity. The role played by thioglycolic acid is not clear. It could adsorb or chemisorb on metal surface, by means of mercapto

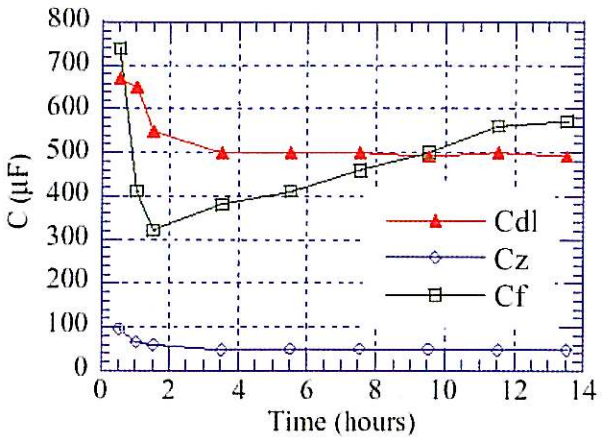


Fig. 11. C_dl, C_f and C_z as a function oftime for a test in inhibitor B at 50 ppm.

(HS$^-$) group or decompose to form FeS that can form an inner layer on which imidazoline can bond heavily. Surface analysis such as FTIR and XPS will be performed to clarify this point.

CONCLUSION

The present paper reports results of the evaluation of the activity of two formulations of imidazoline-based inhibitors for oil field environment.

Data have shown a positive effect of thioglycolic acid on inhibition mechanism. Polarization curves indicated the formation of a protective film, whose desorption potential increase with immersion time and moving from inhibitor A to B. The use of inhibitors permitted reduction of corrosion rates from 1.40 to 0.02 mm/y.

EIS data have been evaluated by three equivalent circuits that permitted the determination of film and charge transfer contribution to total resistance. Two different action mechanisms were detected.

REFERENCES

[1] El Hosary, A. A., *et al.*, 1995. 8 SEIC; Univ. Ferrara, p. 1269.

[2] Choi, H. J., Cepulis R. L., Lee, J. B., 1989. Corrosion, **45**, 943.

[3] *Metals Handbook* ninth edition, 13., p. 1232, ASM International, Metals Park,Ohio.

[4] Tan, Y.J., Bailey S. and Kinsella, B.; 1996. *Corrosion Science* **38**, 1545-1561.

[5] X. Zhang X., Wang F., Y. Du Y. He, Y.; 2001. *Corrosion Science*, **43**, 1417-1431.

[6] Wang D. Ying S. Li Y. *et al.*, 1999.*Corrosion Science* **41**, 1911.

[7] Szyprowski A.J., proceedings of 8 SEIC; 1995. Univ. Ferrara p. 1229.

[8] Edwards A., Osborne C., Webster S. *et al.*; 1993. *Corrosion Science*, **36**, 315.

[9] Wang J., C. Chin Cao, J. 1996. *Soc. Corrosion Protect*, **1**, 69.

[10] Lorenz W.J., Mansfeld F., 1981. *Corrosion Science* **21**, 647.